Influence of the aspect ratio of an additive manufacturing component on the surface roughness during cutting with wire EDM

Influence of the aspect ratio of an additive manufacturing component on the surface roughness during cutting with Wire EDM

Abstract

Aluminum alloy AlSi10Mg is among the most used alloys in powder bed additive technologies with laser source (PBF-LB/M) to make light components in sectors such as aerospace and automotive. These components can have complex shapes and are made in some extrusions directly on the construction platform in order to remove them by wire electrical discharge machining (WEDM) and obtain a surface roughness already suitable to be able to assemble the parts with other components. This study investigated two aspects: the robustness of different instruments for profile and areal roughness measurements on AlSi10Mg parts produced by the PBF-LB/M process; and the effect of the aspect ratio of the components on the surface roughness obtained from WEDM. A better correspondence between the *P*- and *S*- parameters was found than that reported in the literature between the *S*- and *R*- parameters. Analyzing the relationship between weight and height of the AlSi10Mg components, the results showed that the heaviest and tallest component presents the least roughness (Ra = 5.05 µm ± 0.63 µm and Rz = 33.11 µm ± 4.29 µm). However, it emerged that the various areas of the piece have different roughness values (from Ra = 7.65 µm ± 2.85 µm and Rz = 43.07 µm ± 13.12 µm to Ra = 15.21 µm ± 7.37 µm and Rz = 68.39 µm ± 25.75 µm) of and this requires constant adjustment of the cutting parameters to have uniform surface roughness.

Keywords: wire electric discharge machining; additive manufacturing; aluminum alloy; aspect ratio workpiece; surface roughness; laser powder bed fusion.

1. Introduction

Additive manufacturing (AM) technologies allow the production of parts with high design complexity compared to conventional processes [1]. Among these technologies, laser-beam powder bed fusion of metal powder (acronym PBF-LB/M according to ISO/ASTM 59201), is becoming increasingly attractive for the aerospace, automotive and medical industries [2–5]. PBF-LB/M is one of the metal additive technologies that allows, with suitably optimized process parameters, to produce of complex geometries with good dimensional accuracy and surface finish compared to other metal additive technologies. Generally, the components are built on the platform anchored by support structures made of the same material which are also used to hold up the overhanging surfaces and help in the diffusion of heat in order to reduce thermal stresses. In some cases, however, when the geometry permits, it is possible to anchor the part directly to the build platform. The parts can thus be removed mechanically and the surfaces suitable, for example, for assembly with other components can be obtained. One of the most used technologies to carry out the detachment is wire electrical discharge machining (WEDM). WEDM is a spark erosion process using a fine wire electrode of copper, brass or molybdenum to produce complex 2D shapes or cut with accuracy and fine surface roughness electrically conductive workpieces [6, 7]. As with all manufacturing processes, WEDM requires the selection of an appropriate set of machining parameters to achieve the desired material removal and surface roughness. Machine manufacturers generally provide a machinability database to assist the user in making decisions regarding machine settings, electrode wire materials to be used based on the material being cut, etc. These available technological data, which are based on the manufacturer's internal experimentation, are useful but often insufficient when using new metal alloys or non-traditional processes that generate new microstructures and geometries with variable thicknesses. Furthermore, manufacturer guidelines for the selection of processing parameters are conservative and do not always lead to optimal and cost-effective results [8–10]. Numerous researchers have used manufacturing process parameters to obtain a quality product [11–14]. However, there are few studies

related to the WEDM of parts produced in PBF-LB/M and these concern the analysis of samples generally of a parallelepiped shape a few millimetres high. Ozaner et al. [15] investigated WEDM parameters such as pulse on time and pulse off time to analyze their effects on the surface integrity and mechanical characteristics of specimens (starting sample sizes of 40 x 16 x 9 mm) manufactured in PBF-LB/M/Inconel 939. Vaidyaa et al. [16] optimized the WEDM process of PBF-LB/M - fabricated AlSi10Mg produced cuboidal specimen (100 x 100 x 10 mm) through a genetic algorithm approach coupled to a hybrid artificial neural network. Taguchi's experimental design, considering the discharge current, discharge voltage and pulse on time as input factors, is performed to obtain results of microhardness and surface roughness. Franczyk et al. [17] investigated the dependence of both PBF-LB/M and WEDM process parameters on process performance in terms of surface roughness on 7 mm high samples. The machinability of AlSi10Mg + niobium carbide (NbC) composite material, based on the orientation of the pieces during construction with PBF-LB/M process, using the EDM process was investigated by Meghanathan et al. [18].

When components are built directly attached to the build platform, the WEDM cutting is performed by placing the platform vertically so that the wire can cut the part at the desired distance from the build platform. In this way, the piece is equivalent to a beam embedded on one side only. The geometries also produced in PBF-LB/M are lightened at the section level due to thermal stress issues during construction. Also, in some industries such as satellite telecommunications, radio frequency (RF) engineers are increasingly moving towards building monolithic components to reduce issues such as increment mass, volume, and assembling complexity thanks to the diffusion of AM technologies [19–22]. These pieces can therefore come to have a narrow section relative to their height (Fig. 1).

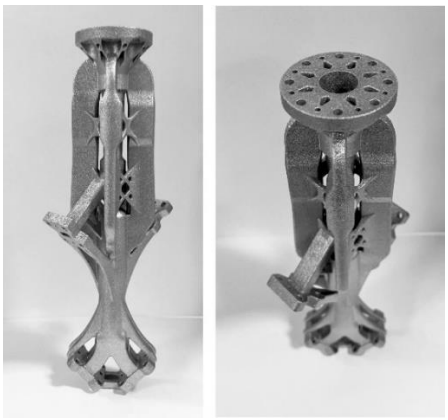

Fig. 1 Example of an RF component: a monolithic K/Ka-Band Dual-Circular Polarization Antenna-Feeding Network [22].

To date, to the authors' knowledge, there are various studies on the improvement of wire EDM accuracy mainly due to wire tension [23–26] and the size of the cutting surface, but there are no studies on the effect of component weight on surface roughness during the WEDM cut. Therefore, the purpose of this study was to analyze the effect of the aspect ratio, in terms of lightness and height of the component, produced in AlSi10Mg alloy with PBF-LB/M technology on surface roughness after WEDM cutting. This is important in order to understand whether it is actually possible to obtain a surface roughness suitable for the application of the component without having to carry out further processing which could be complex based on the complexity of the geometry of the component and therefore of the relative clamping. The cutting process parameters were optimized through a design of experiments (DoE) starting from the data present in the literature. In light of the widespread use of optical profile meters for the analysis of surface irregularities in recent years to verify the specifications of the surface structure on the components made, the need has emerged to be able to make a real comparison with the data reported in the technical drawings. The latter still refer to the specifications of the surface structure of the profile. This has led to scientific questions on how to

compare the profile and areal roughness parameters [27, 28] since the former provide information on profile texture, while the latter describe surface texture in three-dimensional space. For this reason, in this work, the first step was to identify a correspondence between the primary profile (*P*-parameters) and the primary surface (*S*- parameters).

2. Materials and methods

Fig. 2 shows the flowchart of the research process used in this study. Two aspects were investigated: the optimization of cutting parameters and the methodology for compare the profile and areal roughness parameters. The results obtained from a first experimental plan to optimize the cutting parameters for the AlSi10Mg alloy and the identification of the correct cut-off parameter for the measurement of the roughness *R*-parameters were the input for the evaluation of the effect of aspect ratio (lightness and height of the component).

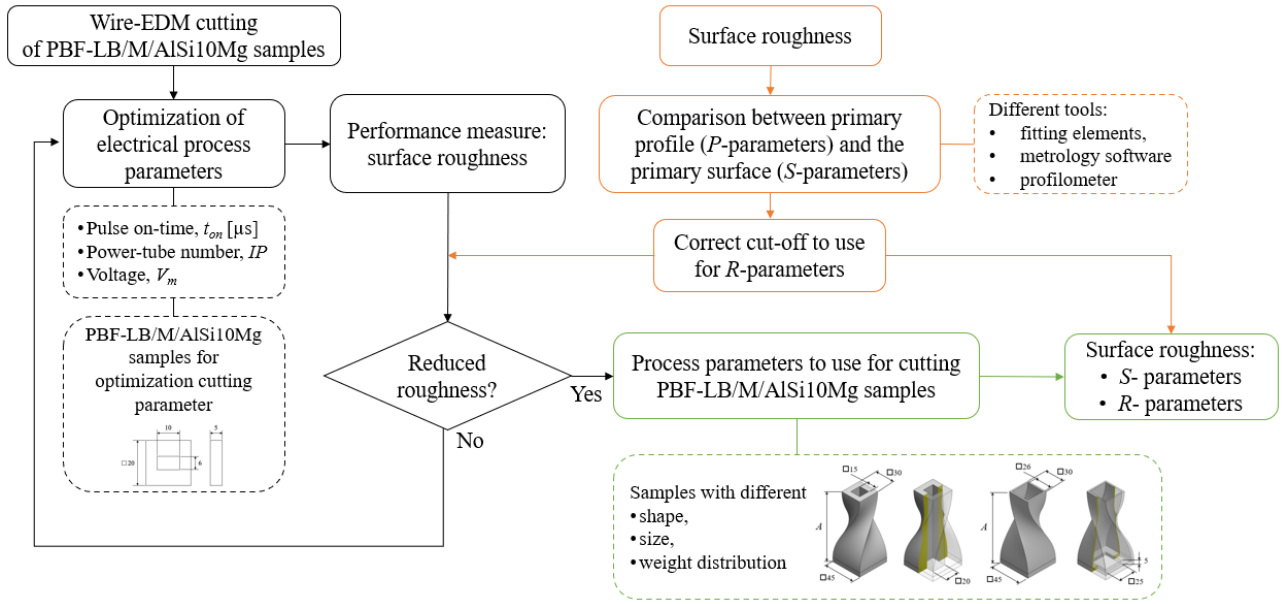

Fig. 2 Flowchart of the of the research process.

2.1 Sample design

To evaluate the influence of cantilever length and sample weight on the roughness in the cut surface, samples with different shape, size and weight distribution were designed (Fig. 3). Samples were manufactured extruded onto the build platform and rotated by 5° relative to the recoater blade to reduce the impact zone between the part and the blade during the layer coating (Fig. 3c).

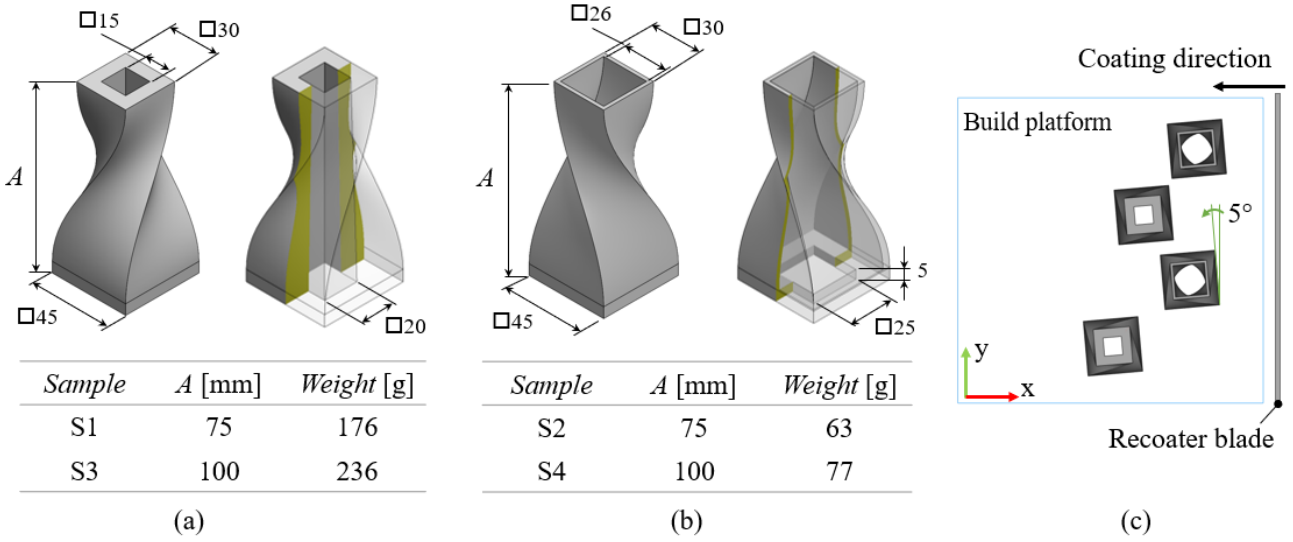

Sample	*A* [mm]	*Weight* [g]
S1	75	176
S3	100	236

(a)

Sample	*A* [mm]	*Weight* [g]
S2	75	63
S4	100	77

(b)

(c)

Fig. 3 (a) Thick and (b) thin samples; (c) samples' position on the build platform.

2.2 Production

Gas-atomized AlSi10Mg powder was used to produce the test specimens. The powders are stored at an ambient temperature of 24°C and a relative atmospheric humidity of 40% as per the manufacturer's instructions. To produce PBF-LB/M/AlSi10Mg (acronym according to ISO/ASTM 59201) test specimens EOSINT M270 Dual Mode (EOS GmbH) system was used, equipped with a 200 W Yb-fiber laser and a beam-spot size of 100 µm. The building platform is heated at 100°C to reduce thermal stresses that arise during the manufacturing process. The machine works in operating conditions at temperatures 25°C - 30°C with a maximum relative atmospheric humidity of 45% as per the manufacturer's instructions. The specimens were produced (Fig. 4) in an argon atmosphere to have an oxygen content of less than 0.10%. Table 1 shows the process parameters used to manufacture the specimens.

	Down-skin	*In-skin (core)*	*Up-skin*	*Contour*
Scan speed [mm/s]	900	800	800	900
Laser power [W]	190	195	190	80
Hatching distance [mm]	0.10	0.17	0.10	-
Layer thickness (mm)	0.03	0.03	0.03	

Table 1. Process parameters values employed for AlSi10Mg sample tests. Down-skin 2 layers; up-skin 3 layers.

As can be seen from Table 1, four different sets of parameter values have been set: with *in-skin or core*, the internal structure of the component has been created; *down-skin* means the lower surfaces in contact with the platform or support structures; with *up-skin* is indicate the final upper surfaces of the component; and finally with *contour* all the contour surfaces. This differentiation allows for improving the quality of the component.

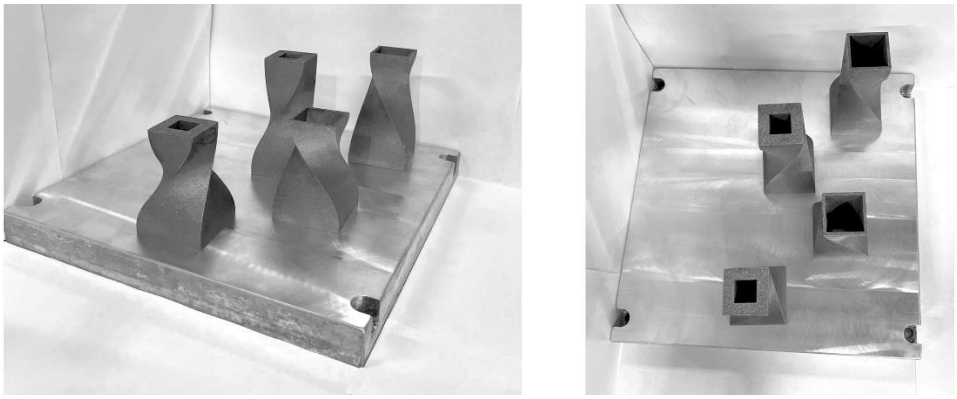

Fig. 4 Test specimens produced.

2.3 Wire EDM machine

The experimental studies in this work were performed on a CNC Wire Cut EDM DK7732 from Suzhou Baoma Numerical Control Equipment. A molybdenum wire-electrode with a diameter of 0.18 mm was used. The temperature range of the machine tool to ensure the working accuracy is 20°C ± 3° with a relative atmospheric humidity of 43% as per the manufacturer's instructions. A first experimental plan was developed to find the best parameters in terms of surface roughness. Fig. 5 and Table 2 show the geometry of the tested samples and the investigated WEDM process parameters, respectively. The current (*IP*) and the machining voltage (V_m) were set at "low" using the proprietary software of the WEDM machine. *IP* means the number of power tubes and it is possible to choose a value from 1 to 6 [29]. If *IP* is larger, the current is larger and the machining speed is faster, however the roughness is worse. For this reason, the lowest *IP* values, 1 and 2, were tested. The "low" setting for the V_m means that the voltage can reach a maximum of 80V as reported by the manufacturer. From the literature [30, 31], it was observed that the pulse off-time (t_{off}) has no significant impact on surface roughness. Therefore, it was been defined according to the manufacturer's calculation chart based on the length of the sample to cut. However, pulse on-time (t_{on}) was tested with values of 10 µs and 15 µs. The working fluid was a JR3A emulsion solution.

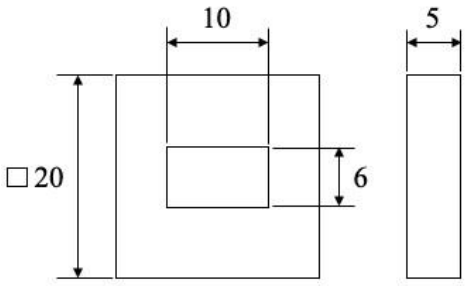

Fig. 5 Geometry of the samples used to optimize the cutting parameters.

Parameters	*Value*
Pulse on-time, t_{on} [µs]	10, 15
Power-tube number, *IP*	1, 2
Voltage, V_m	≤ 80V

Table 2. WEDM process parameters tested in the first experimental plan.

The tests showed a reduction in surface roughness when t_{on} is equal to 10 µs and *IP* is equal to 1. Therefore, these parameters were chosen to evaluate the effect of length and weight of the samples on roughness. Samples designed (Fig. 3) were cut 1.2 mm away from the build platform (Fig. 6).

During cutting, the wire encounters zones of different dimensions, in particular zones a_1, a_2, a_5 and a_6 have a greater area in the *x*-axis than in the *y*-axis, whereas a_3 and a_4 have a smaller dimension in the *x*-axis to the *y*-axis (Fig. 6b). Maintaining the nomenclature of the construction axes and cutting areas, the nomenclature on the surface of the part is mirrored to the surface remaining on the platform (Fig. 6b). This is necessary to avoid interpretation errors during the analysis of the surface on the piece as this is rotated to be able to be analysed.

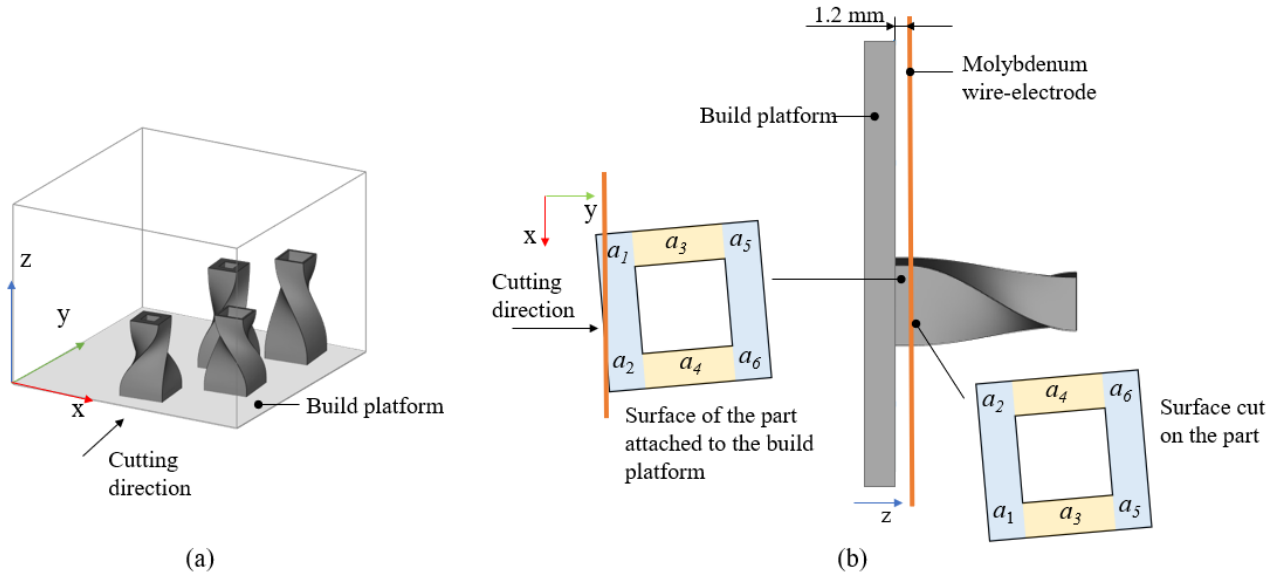

Fig. 6 (a) Cutting direction with respect to manufactured direction; (b) position of the platform during cutting and nomenclature of cutting surfaces.

2.4 Surface roughness

Starting from what is reported in the respective regulations (ISO 21920-2:2022, ISO 25178-2), it is possible to find a correspondence between the primary profile (*P*-parameters) and the primary surface (*S*-parameters). This allows for subsequently tracing the correct cut-off to use instead of carrying out several tests as described in the standard before arriving at the correct value.
Profile parameters have a mathematical expression that can easily be extended to surfaces. For example, the *Sa* equation is the areal extrapolation of the *Ra* (arithmetic mean deviation) equation (Eq.1):

$$Ra = \frac{1}{l}\int_0^l |Z(x)|dx \qquad Sa = \frac{1}{A}\iint_A |Z(x,y)|dxdy \quad (1)$$

Sq, *Ssk*, *Sku*, *Sp*, *Sv*, etc. can therefore be defined straightforwardly in the same way. Parameter equations use integrals instead of sums because they represent the definition for continuous case.
The range of variability of the *S*-parameters was estimated and used to identify the appropriate roughness sampling length (cut-off length). The *P*- and *S*-parameters were compared leading to a better match than that between the *R*- and *S*-parameters. Two different tools were used to estimate the areal roughness parameters, a 3D optical scanner with its 3D analysis software and surface analysis and metrology software. A profilometer was used to estimate the roughness profile parameters. ISO 25178-2 gives some examples of methods for areal topography measurements that include a structured light projection. As indicated by the same international standard, each method used to measure surface roughness, whether they are line-profiling or area-topography, has range and resolution limits both in lateral and vertical directions. The following tools were used to evaluate the roughness:

- SM Metrology Systems RPT80 tester with a diamond stylus of a radius of 2 μm, resolution of 0.001 μm and an accuracy class of 1° according to ISO/DIN with a maximum permissible error of 5%;
- Atos Compact Scan 2M by GOM GmbH, a 3D optical scanner with a resolution of 2MP and accuracy within the expected measurement specifications according to VDI/VDE 2634, Part 3, with the probing error form (PF) of 0.001 mm, probing error size (PS) of -0.004 mm, sphere spacing error (SD) of -0.004 mm and length measurement error (E) of 0.016 mm;
- MountainsMap software by Digital Surf. The software is compliant with ISO 25178 standards.

Three cubic samples in AlSi10Mg produced by PBF/LB/M with side dimensions of 10 mm were used. The up-skin surfaces of the samples were scanned and the areal roughness measurements were performed using two different methodologies: one based on fitting elements (with GOM Inspect software) and the other with surface analysis software (MountainsMap). The up-skin surfaces were analyzed as they present a higher surface and non-periodic roughness compared to the roughness obtainable through WEDM. In this way, the worst condition with the possibility of reflectivity problems due to the greater surface roughness was analysed to evaluate the goodness of the instrumentation used.
As required by ISO 21920-2:2022, the profile trace was detected as an intersection of the leather model with an intersection plane perpendicular to it and in a specified direction (Fig. 7).

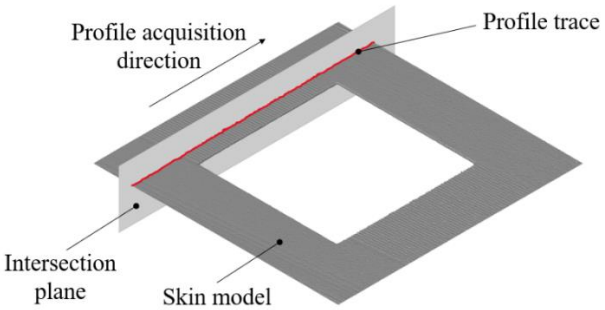

Fig. 7 Profile trace according to ISO 21920-2:2022.

3. Results and discussion

3.1 Surface roughness measurement

For roughness profiles, ISO 21920-2:2022 requires an initial estimate of the roughness profile parameters by visual or surface inspection to select an adequate cut length. Therefore, the areal surface texture method was used as a preliminary analysis to observe the distribution of defects on the surface, identify the range of data variability and select the appropriate cut length for profile measurements. Then, the roughness parameters on the primary profile (*P*-parameters) were evaluated using a profilometer and compared with the primary surface (*S*-parameters).
For the areal surface texture method, the maximum of the deviations was assumed as the maximum value of the peak height *Sp*, the minimum as the maximum value of the depth of the well *Sv*, consequently *Sz* turns out to be the sum of the maximum and the minimum, and finally, the standard deviation of the heights on all points of the geometry was defined as the mean squared height parameter *Sq*. The areal parameters have been used to evaluate the roughness sampling length. The variability range of *Pq*, *Pp* and *Pv* parameters has been identified. *Pz* represents the sum of the largest peak height and the largest pit depth of the primary profile along the sampling length, whereas *Pt* is the same measurement but along the evaluation length. *Pz* values are not available on some commercial profilometers, thus *Pt* has been assumed to be equal to *Sz*.
From the results shown in Table 3, it is evident that both methods (best-fit analysis and metrology software) lead to comparable results with a mean percentage difference of 6%. Fig. 8 shows the color

maps for the two methods used. The histogram of the legends highlights the distribution of irregularities on the surface: the red areas are classified as hilly regions, while the blue areas are valley regions. Both analyses lead to the same chromatic map highlighting the same distribution of points on the reference surface. For the results obtained, the best-fit method was used for the areal surface roughness analysis of the WEDM cut specimens.

The *S*-parameters have been related to the correspondent parameters of the primary profile. In some cases there is an average percentage difference between profile measures and previous analysis of about 20%: it can occur because the lines travelled by the probe can be characterized by more peaks or more pits.

Roughness parameters	*Best-fit analysis*		*Metrology software*		*Primary profile analysis*	
Sample 1	As-built [µm]	Shot-blasted [µm]	As-built [µm]	Shot-blasted [µm]	As-built [µm]	Shot-blasted [µm]
Sq or Pq	42	27	40.4	26.2	49.3 (0.62)	29.5 (1.64)
Sp or Pp	135	95.5	129.6	94	129.1 (5.23)	67.1 (16.44)
Sv or Pv	155	142.5	149.2	137.9	119.9 (7.33)	87.9 (11.01)
St or Pt	290	238	278.9	231.9	249 (4.05)	155 (7.48)
Sample 2	As-built [µm]	Shot-blasted [µm]	As-built [µm]	Shot-blasted [µm]	As-built [µm]	Shot-blasted [µm]
Sq or Pq	48.04	30.7	45.7	30.8	58.89 (3.53)	35.4 (3.26)
Sp or Pp	158.3	98.8	163.4	98.8	131.6 (7.88)	85.6 (5.35)
Sv or Pv	197	146.2	244.6	180.9	159.5 (3.74)	107.1 (12.44)
St or Pt	355.2	245	408	279.7	291.1 (10.64)	192.6 (7.41)
Sample 3	As-built [µm]	Shot-blasted [µm]	As-built [µm]	Shot-blasted [µm]	As-built [µm]	Shot-blasted [µm]
Sq or Pq	51.8	33.1	50.3	32.1	52.9 (3.34)	40 (2.96)
Sp or Pp	151.2	90.6	152.9	86.3	132.5 (23.11)	77.7 (0.39)
Sv or Pv	197.8	168.4	215.1	187.2	145.6 (12.27)	116.6 (8.87)
St or Pt	349	259	368	273.5	278.2 (30.43)	194.4 (8.83)

Table 3. Comparison between primary surface and primary profile measurements. Standard deviation in parentheses.

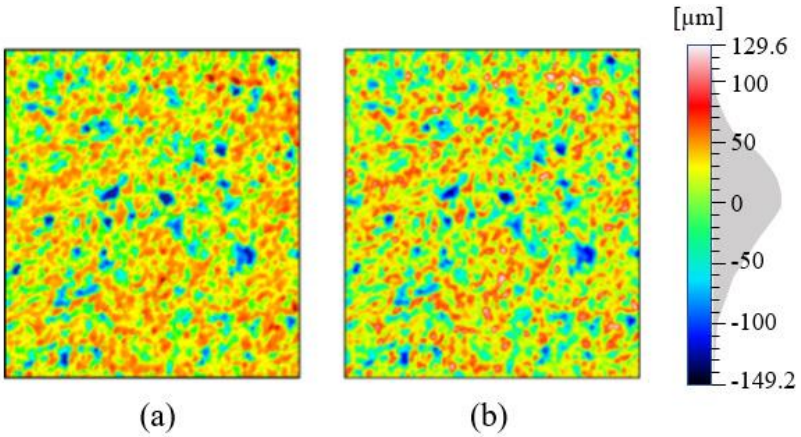

Fig. 8 Color map of sample 1: surfaces obtained with (a) GOM Inspect and (b) MountainsMap.

The *Pt* parameter thus makes it possible to go back to the setting class according to ISO 21920-3:2022 and obtain the correct evaluation length.

3.2 Effect of the aspect ratio on roughness

Table 4 and Fig. 9 show the areal roughness results: it can be deduced that S3 has a greater roughness localized in area a_4. This leads to thinking that the greater length and greater weight result in worse surface roughness on half of the surface. Observing the Gaussian distribution of Fig. 9, it can be seen that it is very close in samples S2 and S4 while it has a slightly larger amplitude in samples S1 and S3.

Samples	*Sq* [µm]	*Sp* [µm]	*Sv* [µm]	*St* [µm]
S1	31.58	113.82	278.48	392.30
S2	32.22	113.37	317.78	431.15
S3	38.80	236.79	266.08	502.87
S4	32.66	50.53	271.24	321.77

Table 4. Areal surface roughness values.

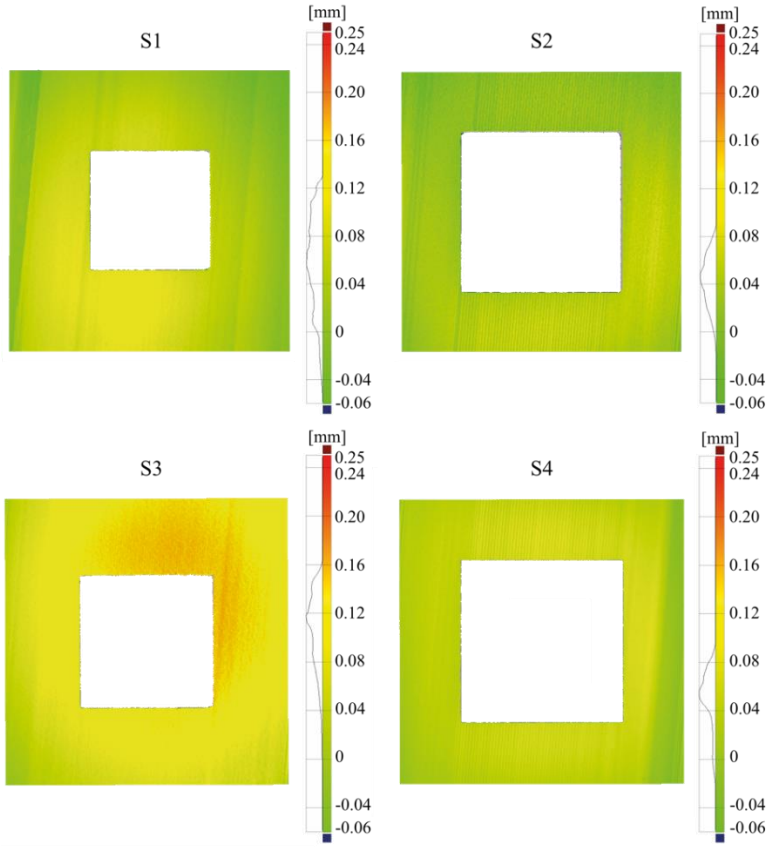

Fig. 9 Color map of surfaces with Gaussian distribution.

The range of *S*-parameters suggests using a cut-off of 8 mm which by standard implies an evaluation length of 40 mm considering the number of sections equal to 5. When looking at the six zones within the part surface, there is not enough space in all areas to carry out measurements. By making a comparison between the measurements carried out with the evaluation length and five individual sampling lengths along the evaluation length, in the first case, the profilometer averaged the measurements of the single sampling lengths. Consequently, even if there is not enough area on the surface to be analysed to cover the total evaluation length, it is sufficient to perform several measurements with the sampling length and reach the total evaluation length. Table 5 shows the results in terms of *Ra* and *Rz*.

Samples	a_1		a_2		a_3		a_4		a_5		a_6	
	Ra	*Rz*	*Ra*	*Rz*	*Ra*	*Rz*	*Ra*	*Rz*	*Ra*	*Rz*	*Ra*	*Rz*
S1	11.34 (0.41)	60.79 (4.94)	10.66 (0.67)	54.56 (2.08)	18.05 (0.16)	81.09 (2.42)	19.23 (0.84)	85.34 (1.99)	10.45 (0.47)	55.69 (4.17)	10.32 (0.49)	56.68 (6.51)
S2	9.17 (0.30)	51.77 (1.69)	9.68 (0.36)	53.94 (0.64)	19.54 (0.71)	83.24 (6.52)	21.99 (0.63)	90.25 (2.88)	9.37 (0.43)	50.64 (2.85)	10.48 (0.57)	55.95 (2.17)
S3	4.68 (0.25)	30.28 (3.41)	5.02 (0.50)	34.81 (4.26)	5.48 (0.20)	36.11 (1.49)	5.20 (0.16)	33.65 (3.79)	4.07 (0.38)	26.04 (1.09)	5.90 (0.03)	37.78 (1.13)
S4	7.92 (0.14)	43.00 (1.49)	8.74 (0.37)	48.20 (2.27)	8.27 (0.44)	45.07 (1.82)	14.44 (0.88)	64.31 (4.11)	6.73 (0.54)	39.90 (5.20)	5.22 (0.15)	35.42 (3.84)

Table 5. Results of the profile surface roughness. The values are in [µm]. The standard deviation is indicated in parentheses.

Compared to the analysis of areal surface roughness, the results allow for a more in-depth analysis of the effect of height and weight during cutting. Fig. 10 shows the factor plots. The main effects plot (Fig. 10a) shows the relationship between surface roughness and the individual variables, that are area on the surface (*zone*), height (*A*) and weight (*weight*); the interaction plot (Fig. 10b) visualizes how the relationship between one variable and roughness depends on the value of a second variable. Fig. 10c shows the 3D surface plot from which it can be seen how the roughness variable relates to the two variables height and weight. The peaks and valleys correspond to combinations of heights and weights that produce local maxima and minima, respectively.

As evidenced by the surface analysis, zones a_3 and a_4 are those in which there is a greater variation in the roughness trend. In general, looking at the main plot (Fig. 10a), the taller samples show a lower roughness and, except in the case of the component with a weight of 77 g, the roughness of the heavier samples is almost similar to the roughness of the sample lighter. Observing the interaction between zone and height (Fig. 10b), it can be seen that the lowest samples in addition to having a higher average roughness, show a sudden increase in roughness passing from zone a_2 to zone a_3 and a sudden decrease from zone a_4 to zone a_5. In the case of the highest samples, there is no sudden variation of roughness in those areas but there is a greater roughness in area a_4 as evidenced by the areal roughness. Analyzing the relationship between weight and height (Fig. 10c), it is evident that the heaviest and tallest component (S3) has the lowest roughness. This is mainly due to if the component is considered as a beam blocked only at one end, the higher and heavier it is, the more it will tend to open, also due to the force of gravity which adds up to the weight, as the electrode advances thus leading to the creation of a gap which improves the surface roughness (Fig. 11). Since the component is built with an inclination of 5°, the opening of the component will be incremental and not clear on the final length of the surface. The zone a_4 has a greater roughness because the sample, while it opens more from the top, in the lower area will tend to close, reducing the gap and therefore worsening the roughness.

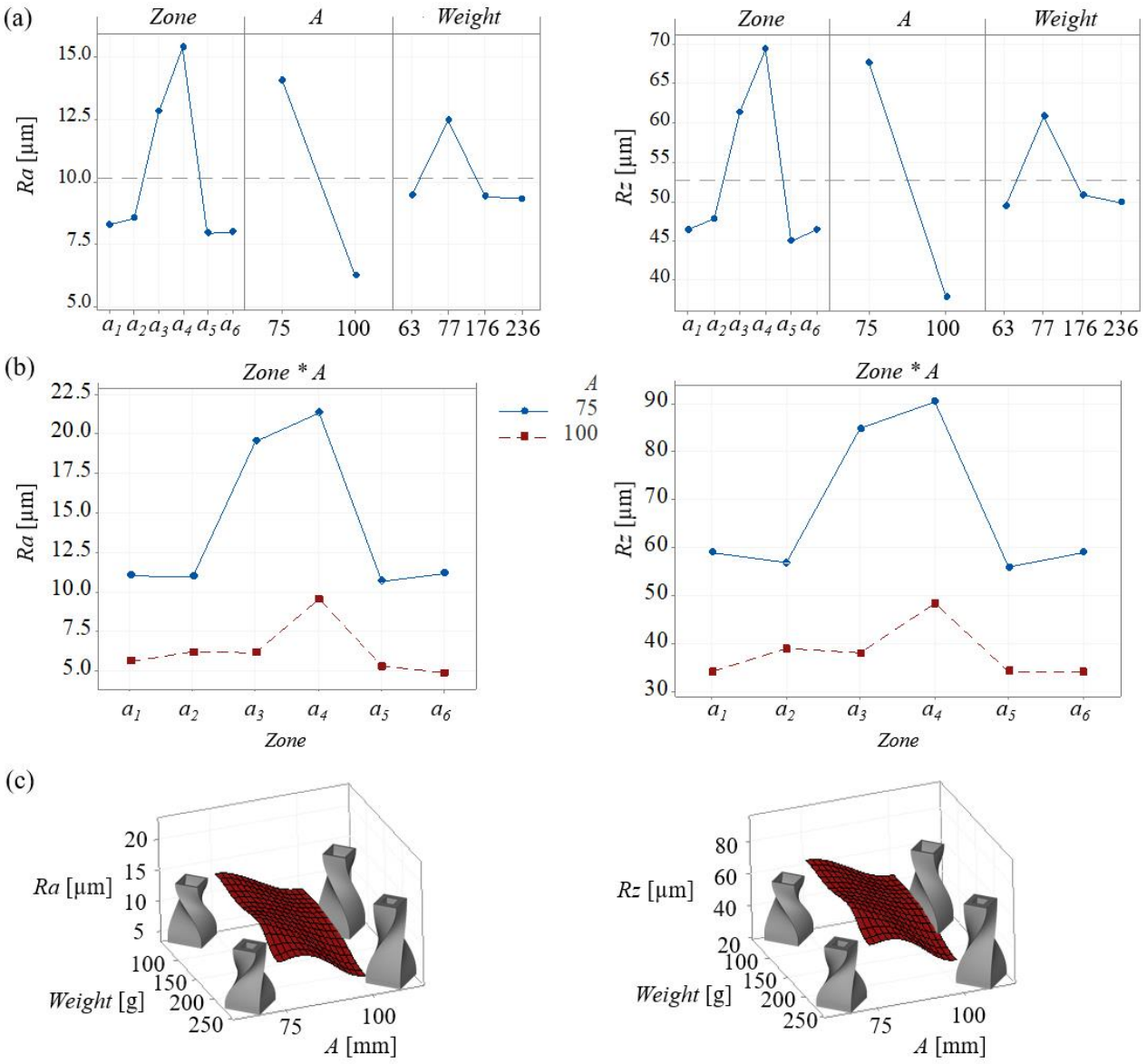

Fig. 10 (a) Main effects plot, (b) interaction plot, and (c) surface plot for *Ra* and *Rz*.

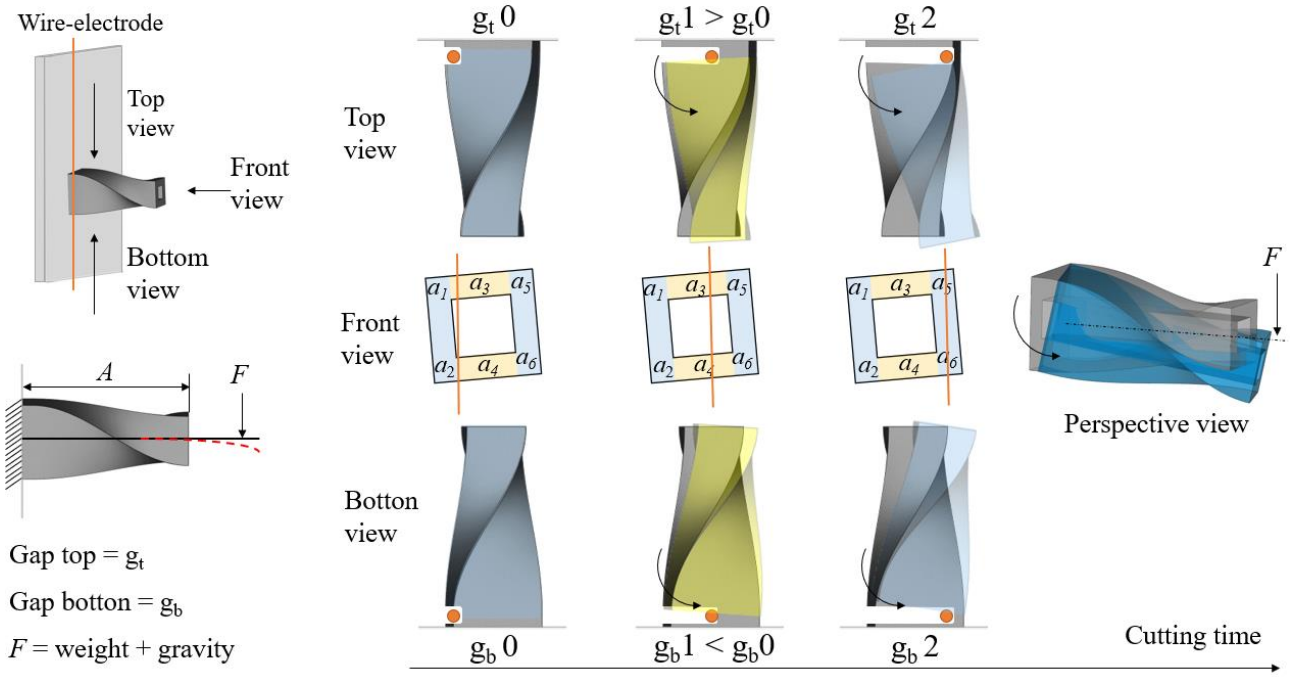

Fig. 11 Diagram of the rotation of the S3 and S4 samples during cutting.

The variable surface that can be found in a piece manufactured with PBF-LB/M technologies implies the need for a constant adjustment of the parameters to arrive at a more uniform surface roughness on the surface of the piece. However, it is interesting to note that the profile roughness measurements bring out the effect of the aspect ratio on the final roughness of the component more clearly than the areal roughness measurements. In fact, with the same cutting surface, the S1 component has a greater roughness than the S3 component probably because the protrusion effect (height) added to the gravity and weight in the S1 sample is lower than in the case of the S3 sample. Sample S4 also has a lower roughness than sample S2, highlighting the positive effect due to the height with the same cut surface.

4. Conclusion

The study focused on two aspects: the first concerned the possibility of comparing the area and the profile of the roughness with different tools (one based on fitting elements, a metrology software (e.g.MountainsMap) and a profilometer), and the second was the effect of the aspect ratio on the roughness obtained by cutting using WEDM of pieces made with an additive process. The following conclusions can be deduced:

- the two methods tested for areal surface analysis (best-fit analysis and metrology software) led to similar results with a percentage difference of about 6%;
- from areal surface texture analysis, it was possible to identify the zones with more defects and the cut-off length for profile measurements;
- it is possible to use the sampling length as evaluation length for profile roughness measures;
- a better correlation has been found between *S*- and *P*- parameters, instead of the main reported in the literature between *S*- and *R*- parameters;
- analyzing the samples with the same cutting length, due to the force understood as the sum of the weight of the object itself and gravity, the taller and heavier components show better surface roughness considering *R*-parameters (S3: *Ra* = 5.05 µm ± 0.63 µm and *Rz* = 33.11 µm ± 4.29 µm). In contrast, the lightest and lowest component (S2) has the highest roughness (*Ra* = 13.37 µm ± 5.8 µm and *Rz* = 64.30 µm ± 17.62 µm);
- the surface of a PBF-LB/M component can present variable sections which imply the need for a constant adjustment of the parameters to arrive at a more uniform surface roughness on the surface of the piece;

- profile roughness measurements show more effect of the aspect ratio on the final roughness of the component than areal roughness measurements.

Declaration of Competing Interest

The authors declare that they have no known competing financial interests or personal relationships that could have appeared to influence the work reported in this paper.

References

1. Gibson, I., Rosen, D.W., Stucker, B.: Additive Manufacturing Technologies, Springer (2010). (2014)
2. Calignano, F., Manfredi, D., Ambrosio, E.P., Biamino, S., Lombardi, M., Atzeni, E., Salmi, A., Minetola, P., Iuliano, L., Fino, P.: Overview on additive manufacturing technologies. Proc. IEEE. 105, 593–612 (2017). https://doi.org/10.1109/JPROC.2016.2625098
3. Tepylo, N., Huang, X., Patnaik, P.C.: Laser-Based Additive Manufacturing Technologies for Aerospace Applications, (2019)
4. Delic, M., Eyers, D.R.: The effect of additive manufacturing adoption on supply chain flexibility and performance: An empirical analysis from the automotive industry. Int. J. Prod. Econ. (2020). https://doi.org/10.1016/j.ijpe.2020.107689
5. Bidare, P., Jiménez, A., Hassanin, H., Essa, K.: Porosity, cracks, and mechanical properties of additively manufactured tooling alloys: a review. Adv. Manuf. (2022). https://doi.org/10.1007/s40436-021-00365-y
6. Ho, K.H., Newman, S.T., Rahimifard, S., Allen, R.D.: State of the art in wire electrical discharge machining (WEDM). Int. J. Mach. Tools Manuf. 44, 1247–1259 (2004)
7. Camposeco-Negrete, C.: Analysis and optimization of sustainable machining of AISI O1 tool steel by the wire-EDM process. Adv. Manuf. (2021). https://doi.org/10.1007/s40436-021-00353-2
8. Scott, D., Boyina, S., Rajurkar, K.P.: Analysis and optimization of parameter combinations in wire electrical discharge machining. Int. J. Prod. Res. (1991). https://doi.org/10.1080/00207549108948078
9. Asgar, M.E., Singholi, A.K.S.: Parameter study and optimization of {WEDM} process: A Review. {IOP} Conf. Ser. Mater. Sci. Eng. 404, 12007 (2018). https://doi.org/10.1088/1757-899x/404/1/012007
10. Singh, H., Garg, R.: Effects of process parameters on material removal rate in WEDM. J. Achiev. Mater. Manuf. Eng. (2009)
11. Goyal, A., Ur Rahman, H.: Experimental studies on Wire EDM for surface roughness and kerf width for shape memory alloy. Sadhana - Acad. Proc. Eng. Sci. (2021). https://doi.org/10.1007/s12046-021-01684-3
12. Naeim, N., AbouEleaz, M.A., Elkaseer, A.: Experimental Investigation of Surface Roughness and Material Removal Rate in Wire EDM of Stainless Steel 304. Materials (Basel). (2023). https://doi.org/10.3390/ma16031022

13. Ram, H.S., Uthayakumar, M., Kumar, S.S., Kumaran, S.T., Azzopardi, B., Korniejenko, K.: Prediction of Kerf Width and Surface Roughness of Al6351 Based Composite in Wire-Cut Electric Discharge Machining Using Mathematical Modelling. Materials (Basel). (2022). https://doi.org/10.3390/ma15031102

14. Galati, M., Antonioni, P., Calignano, F., Atzeni, E.: Experimental Investigation on the Cutting of Additively Manufactured Ti6Al4V with Wire-EDM and the Analytical Modelling of Cutting Speed and Surface Roughness. J. Manuf. Mater. Process. (2023). https://doi.org/10.3390/jmmp7020069

15. Ozaner, O.C., Dursun, G., Akbulut, G.: Effects of wire-EDM parameters on the surface integrity and mechanical characteristics of additively manufactured Inconel 939. In: Materials Today: Proceedings (2021)

16. Vaidyaa, P., John, J.J., Puviyarasan, M., Prabhu, T.R., Prasad, N.E.: Wire EDM Parameter Optimization of AlSi10Mg Alloy. Trans. Indian Inst. Met. (2021). https://doi.org/10.1007/s12666-021-02344-0

17. Franczyk, E., Machno, M., Zębala, W.: Investigation and optimization of the slm and wedm processes' parameters for the AlSi10Mg-sintered part. Materials (Basel). 14, 1–16 (2021). https://doi.org/10.3390/ma14020410

18. Meghanathan, S., Radhakrishnan, R.M., Ramamoorthi, V., Srinivasan, R.: Machinability study on laser-based powder bed fusion processed hypo-eutectic aluminium alloy composite (AlSi10Mg + NbC). Proc. Inst. Mech. Eng. Part L J. Mater. Des. Appl. (2023). https://doi.org/10.1177/14644207231192812

19. Calignano, F., Peverini, O.A., Addamo, G., Iuliano, L.: Accuracy of complex internal channels produced by laser powder bed fusion process. J. Manuf. Process. (2020). https://doi.org/10.1016/j.jmapro.2020.02.045

20. Sorrentino, R., Peverini, O.A.: Additive manufacturing: A key enabling technology for next-generation microwave and millimeter-wave systems [point of view], (2016)

21. Laplanche, E., Feuray, W., Sence, J., Perigaud, A., Tantot, O., Delhote, N., Menudier, C., Arnaud, E., Thevenot, M., Monédière, T., Passerieux, D., Verdeyme, S., Bila, S., Baillargeat, D., Carpentier, L.: Additive manufacturing of low cost and efficient proof of concepts for microwave passive components. IET Microwaves, Antennas Propag. (2017). https://doi.org/10.1049/iet-map.2017.0157

22. Addamo, G., Lumia, M., Calignano, F., Paonessa, F., Virone, G., Manfredi, D., Iuliano, L., Peverini, O.A.: 3D Printing of a Monolithic K/Ka-Band Dual-Circular Polarization Antenna-Feeding Network. IEEE Access. (2021). https://doi.org/10.1109/ACCESS.2021.3089826

23. Sarkar, S., Sekh, M., Mitra, S., Bhattacharyya, B.: A novel method of determination of wire lag for enhanced profile accuracy in WEDM. Precis. Eng. (2011). https://doi.org/10.1016/j.precisioneng.2011.01.001

24. Yan, M.T., Huang, P.H.: Accuracy improvement of wire-EDM by real-time wire tension control. Int. J. Mach. Tools Manuf. (2004). https://doi.org/10.1016/j.ijmachtools.2004.01.019

25. Puri, A.B., Bhattacharyya, B.: An analysis and optimisation of the geometrical inaccuracy due to wire lag phenomenon in WEDM. Int. J. Mach. Tools Manuf. (2003). https://doi.org/10.1016/S0890-6955(02)00158-X

26. Sanchez, J.A., De Lacalle, L.N.L., Lamikiz, A.: A computer-aided system for the optimization

of the accuracy of the wire electro-discharge machining process. Int. J. Comput. Integr. Manuf. (2004). https://doi.org/10.1080/09511920310001626590

27. Harcarik, M., Jankovych, R.: Relationship between values of profile and areal surface texture parameters. MM Sci. J. (2016). https://doi.org/10.17973/MMSJ.2016_12_2016206

28. He, B., Ding, S., Shi, Z.: A comparison between profile and areal surface roughness parameters. Metrol. Meas. Syst. (2021). https://doi.org/10.24425/mms.2021.137133

29. Xu, J., Xia, K., Lian, Z., Zhang, L., Yu, H., Yu, Z., Weng, Z., Wang, Z.: Surface properties on magnesium alloy and corrosion behaviour based high-speed wire electrical discharge machine power tubes. Micro Nano Lett. (2016). https://doi.org/10.1049/mnl.2015.0204

30. Sridhar Reddy, B., Koteswara Rao, A.B., Ranga Janardhana, G.: Multi-objective optimization of surface roughness, recast layer thickness and surface crack density in WEDM of Al2124/SiCpusing desirability approach. Mater. Today Proc. 39, 1320–1326 (2020). https://doi.org/10.1016/j.matpr.2020.04.563

31. Wasif, M., Ahmed Khan, Y., Zulqarnain, A., Amir Iqbal, S.: Analysis and optimization of wire Electro-Discharge Machining process parameters for the efficient cutting of Aluminum 5454 alloy. Alexandria Eng. J. 61, 6191–6203 (2022). https://doi.org/10.1016/j.aej.2021.11.048